

Improve observation-based ground-level ozone spatial distribution by compositing satellite and surface observations: A simulation experiment



Yuzhong Zhang^{a,*}, Yuhang Wang^a, James Crawford^b, Ye Cheng^a, Jianfeng Li^a

^a School of Earth and Atmospheric Sciences, Georgia Institute of Technology, Atlanta, GA 30332, USA

^b NASA Langley Research Center, Hampton, VA 23681, USA

ARTICLE INFO

Keywords:

Surface ozone
Indirect satellite retrieval
Formaldehyde
Nitrogen dioxide
Geostationary satellite

ABSTRACT

Obtaining the full spatial coverage of daily surface ozone fields is challenging because of the sparsity of the surface monitoring network and the difficulty in direct satellite retrievals of surface ozone. We propose an indirect satellite retrieval framework to utilize the information from satellite-measured column densities of tropospheric NO₂ and CH₂O, which are sensitive to the lower troposphere, to derive surface ozone fields. The method is applicable to upcoming geostationary satellites with high-quality NO₂ and CH₂O measurements. To prove the concept, we conduct a simulation experiment using a 3-D chemical transport model for July 2011 over the eastern US. The results show that a second order regression using both NO₂ and CH₂O column densities can be an effective predictor for daily maximum 8-h average ozone. Furthermore, this indirect retrieval approach is shown to be complementary to spatial interpolation of surface observations, especially in regions where the surface sites are sparse. Combining column observations of NO₂ and CH₂O with surface site measurements leads to an improved representation of surface ozone over simple kriging, increasing the R² value from 0.53 to 0.64 at a surface site distance of 252 km. The improvements are even more significant with larger surface site distances. The simulation experiment suggests that the indirect satellite retrieval technique can potentially be a useful tool to derive the full spatial coverage of daily surface ozone fields if satellite observation uncertainty is moderate.

1. Introduction

Ozone (O₃) in the boundary layer is mainly produced from the photochemical reactions of nitrogen dioxide (NO₂) and volatile organic compounds (VOC). Harmful to the health of human (Brunekreef and Holgate, 2002) and vegetation (Reich and Amundson, 1985), ozone near the surface has long been thought as an air pollution concern. Information on surface ozone with a full spatial coverage are important for evaluating the ozone exposure to human and vegetation (Avneri et al., 2011; Zou et al., 2009). However, the current ground-based monitoring networks do not provide adequate information to represent the spatial distribution of surface ozone, especially in rural or remote areas. Although there are monitoring networks designed to represent the regional background (e.g., CASTNET), their sites are often too sparse to capture the spatial variability in many regions.

Alternatively, satellite-based observations can provide good spatial coverages. For example, satellite observed aerosol optical depth has been applied to derive daily “gap-free” surface PM_{2.5} field (Lv et al., 2016). Satellite can measure ozone in ultraviolet (UV) and thermal infrared (TIR) bands. However, because of molecular scattering in the

UV (Liu et al., 2005, 2010) and lack of thermal contrast in the TIR (Beer, 2006), the satellite instruments are insensitive to ozone in the lower troposphere, posing challenges to the direct retrieval of surface ozone fields from satellite measurements. Multispectral techniques, such as UV + TIR (Worden et al., 2007; Zoogman et al., 2014a) and UV plus visible band (560–620 nm) (Liu et al., 2005; Zoogman et al., 2014a), are proposed to improve the sensitivity to the lower tropospheric ozone. Joint assimilation of ozone and carbon monoxide (CO) is also proposed to improve surface ozone retrieval by exploiting the ozone-CO model error correlations (Zoogman et al., 2014b). But these techniques have not been extensively tested in operation.

Recent aircraft measurements during the Deriving Information on Surface Conditions from Column and Vertically Resolved Observations Relevant to Air Quality (DISCOVER-AQ) campaign show that surface ozone concentration correlates well with tropospheric column densities of nitrogen dioxide (NO₂), a major component of NO_x (NO + NO₂), and formaldehyde (CH₂O), a major product from the oxidation of VOCs including biogenic isoprene (Cheng et al., 2017; Schroeder et al., 2016) (Also see Fig. 3). The O₃-NO₂ and O₃-CH₂O relationships shown in the measurements are broadly consistent with the current understanding of

* Corresponding author. 29 Oxford St., Cambridge, MA 02138, USA.

E-mail address: yuzhongzhang@seas.harvard.edu (Y. Zhang).

¹ Now at School of Engineering and Applied Sciences, Harvard University, Cambridge, MA 02138, USA.

ozone photochemistry (i.e., boundary layer O_3 is mainly produced from reactions of NO_x and VOCs at the presence of sunlight). In addition, previous studies have used the ratios between satellite-observed CH_2O and NO_2 columns to diagnose the ozone production regime (Martin et al., 2004; Duncan et al., 2010; Jin and Holloway, 2015), suggesting that these column measurements contain information for surface O_3 .

Unlike ozone, which has relatively small vertical gradient in the troposphere, NO_2 and CH_2O are usually enhanced in the boundary layer and this enhancement can easily be observed by satellites (e.g., Boersma et al., 2011; Zhu et al., 2016). Hence, it may be feasible to derive surface ozone indirectly from satellite tropospheric NO_2 and CH_2O column densities. This “indirect satellite retrieval” (ISR) approach requires good-quality NO_2 and CH_2O column density retrievals. Partly because the return time of polar-orbiting satellites is at most once per day, current daily retrievals of NO_2 and CH_2O column densities usually have a high noise level and are therefore not suitable for the ISR method. However, the planned constellation of geostationary satellites, TEMPO over North America (Chance et al., 2013), SENTINEL-4 over Europe (Ingmann et al., 2012), and GEMS over East Asia (Bak et al., 2013), should be able to greatly reduce the noise in the satellite column density retrievals on a daily basis. For example, the baseline retrieval products of TEMPO are designed to have precision of about 0.5×10^{15} molecules cm^{-2} for NO_2 and about 2×10^{15} molecules cm^{-2} for CH_2O (Chance et al., 2013). It is reasonable to expect that the indirect retrieval method using tropospheric NO_2 and CH_2O measurements by future geostationary satellites may provide useful information for the distribution of surface ozone.

In this study, we will outline the framework of the ISR method. We will also conduct a simulation experiment using the outputs from a 3-D chemical transport model to study the factors that affect the performance of the ISR method and evaluate whether this new technique may add values to the existing surface ozone monitoring networks.

2. Methodology

2.1. Indirect satellite retrieval (ISR) framework

We examine the feasibility of “retrieving” surface ozone indirectly from satellite tropospheric NO_2 and CH_2O column observations, both of which have good satellite measurement sensitivities in the boundary layer. Fig. 1 illustrates the framework of the “indirect satellite retrieval” (ISR) method in three steps: 1) construct a surface ozone predictor to relate surface ozone mixing ratios with tropospheric NO_2 and CH_2O column densities; 2) predict the full spatial coverage surface ozone mixing ratio field using satellite NO_2 and CH_2O column data with the predictor established in Step 1, and 3) correct the surface ozone mixing ratio field predicted in Step 2 with ground-based observations. We use a linear regression model as the surface ozone predictor in Step 1. The linear model will be derived from surface site O_3 observations and corresponding satellite observations over the surface sites. More sophisticated methods, such as a formal assimilation system, can also be used to replace the linear regression model used in this study. It is also

noteworthy that Step 3 (i.e., post-correction with ground-based observations) is optional. However, we show in Section 3.2 that incorporating information from surface measurements reduces regional-scale biases and greatly improves the performance of surface ozone prediction.

2.2. Simulation experiment

To test whether future high-quality satellite NO_2 and CH_2O observations can be useful for deriving surface ozone concentrations, we setup a simulation experiment to conduct the ISR method outlined in Section 2.1. Similar to an Observing System Simulation Experiment (OSSE), which is a widely-used technique for assessing the added value of a new satellite instrument to an existing observing system (Timmermans et al., 2015), we regard the simulated fields from a 3-D chemical transport model (CTM) (Section 2.3) as the “true” state of the atmosphere and apply the ISR method to the synthetic fields. Unlike a standard OSSE, which usually uses a second 3-D CTM as the “forward model” for assimilation (Zoogman et al., 2011), we use the simple statistical relationship to derive surface ozone from column observations. The focus here is to demonstrate the predictability of surface ozone using column NO_2 and CH_2O data rather than to construct a formal assimilation system.

Conceptually, NO_2 and CH_2O should contain more information about surface ozone when ozone production from NO_x and VOCs is significant. The ISR method is expected to work during warm seasons over regions with significant emissions of ozone precursors. Therefore, the simulation experiment is conducted over the eastern US for July 2011. The procedure follows the ISR framework described in Section 2.1 and is described in details as follows:

- 1 Define hypothetical surface sites in the model domain. For simplicity, these hypothetical surface sites are always defined in the center of a model grid and spaced regularly in both east-west and north-south directions. The surface site distance (i.e., the distance between two nearest surface sites), referred to as SSD hereafter, is varied from 72 km to 720 km to test the impact of the surface site density on the performance (see Section 3.3).
- 2 Construct a statistical model to predict surface ozone. We use pseudo-observations from the model at the predefined hypothetical surface sites to establish statistical relationships between surface ozone concentrations (daily maximum 8-h averages) and co-located tropospheric NO_2 and CH_2O column densities (daily values around 1:00 p.m. local time). All pseudo-observations during July 2011 are lumped together to fit a regression model and the resulting relationship is applied to the whole domain in Step 3. To ensure the robustness of the linear regression model, the tropospheric NO_2 column densities with a heavy-tailed distribution are first log-transformed before applying to linear regression. To study the predictability of column densities, various combinations of predictors are tested (Table 1). For example, in the statistical models named “ CH_2O ” and “ NO_2 ” (Table 1), either CH_2O or log-transformed NO_2

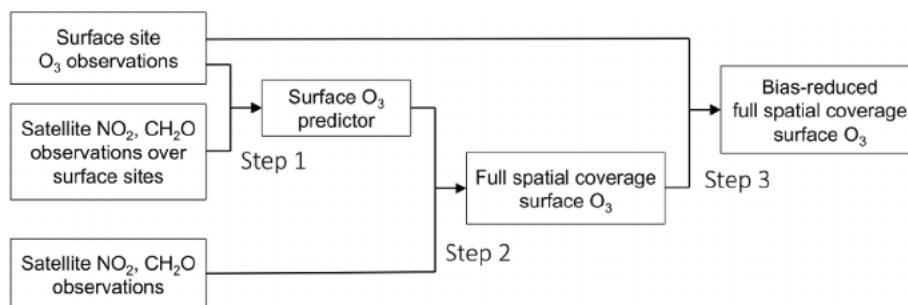


Fig. 1. Framework of the ISR method to derive surface ozone spatial distribution using satellite tropospheric NO_2 and CH_2O column observations and surface site ozone observations.

Table 1
Statistical model for variations of the ISR method.

Name	Statistical model
CH ₂ O	$Y \sim X_1$
NO ₂	$Y \sim X_2$
Linear	$Y \sim X_1 + X_2$
Full	$Y \sim (X_1 + X_2)^2 + X_1 + X_2$
CH ₂ O + SI	$Y \sim X_1$; Correct with simple kriging (Y)~1
NO ₂ + SI	$Y \sim X_2$; Correct with simple kriging (Y)~1
Linear + SI	$Y \sim X_1 + X_2$; Correct with simple kriging (Y)~1
Full + SI	$Y \sim (X_1 + X_2)^2 + X_1 + X_2$; Correct with simple kriging (Y)~1
SI	Simple kriging $Y \sim 1$

columns are used as predictors for surface ozone, whereas in the statistical model named “Linear”, both predictors, CH₂O and log-transformed NO₂ columns, are used. In the statistical model “Full”, we further add second-order terms of CH₂O or log-transformed NO₂ columns (including interactions between the two variables) to account for their non-linearity effects on surface ozone. Section 3.1 discusses the performance of varied statistical predictors. This step can be thought as statistically training a forward model using the historic surface and satellite observations.

- Indirectly retrieve surface ozone mixing ratios. We apply the derived statistical relationships to the whole domain to compute the surface ozone fields (daily maximum 8-h averages) over eastern US based on daily column observations of NO₂ and/or CH₂O. Because of the factors that cannot be resolved in a simple linear model, the errors in these derived surface ozone fields often feature spatial patterns (See Section 3.2). To reduce these errors, we spatially interpolate (simple kriging) the correction term found at the hypothetical surface sites (difference between surface ozone observations and ozone mixing ratios derived from regression) and apply the correction over the entire domain. This post-correction approach is similar to Lv et al. (2016), in which the authors derived surface PM_{2.5} fields from satellite AOD and surface site PM_{2.5} observations. By spatially interpolating the correction at surface sites, we effectively incorporate the information from the surface observations into the final results. We hereafter denote the results using this technique with a postfix “+SI” (e.g., Full + SI), which stands for spatial interpolation.
- Evaluate the results. We evaluate the surface ozone mixing ratios (daily maximum 8-h averages) computed from different variations of the ISR method against the “true” values from model outputs with two performance metrics, Pearson’s correlation coefficient (*r*) and root mean squared error (RMSE). Results over the hypothetical surface sites are excluded in the evaluation. We also compute the performance metrics for spatially interpolating surface ozone observations at hypothetical surface sites using simple kriging. These cases are denoted as “SI”. Results in Section 3.2 show that column observations of NO₂ and CH₂O have potential to add values to existing ground-based observations.

In the simulation experiment described above, we use the model simulated NO₂ and CH₂O column densities, which can be thought as perfectly accurate satellite observations. In reality, satellite observations are subject to varied uncertainties. To assess the impact of satellite observation uncertainties, we perform additional calculations with random errors added to the CTM-simulated tropospheric NO₂ and CH₂O column densities. The random errors are assigned to be normally distributed with zero mean and standard deviations of 0.5×10^{15} molecules cm⁻² for NO₂ and 2×10^{15} molecules cm⁻² for CH₂O, consistent with precision specification in the TEMPO baseline retrieval products (Chance et al., 2013). Section 3.4 discusses the impact of satellite observation uncertainties on the performance of the ISR method.

2.3. Chemical transport model

We use the 3-D Regional chEmical trAnsport Model (REAM) for the simulation experiment described in Section 2.2. The REAM has been successfully applied to study the NO_x-hydrocarbon-O₃ chemistry (Choi et al., 2008; Zhao et al., 2010; Zhang and Wang, 2016; Zhang et al., 2017) and satellite emission inversions (Zhao and Wang, 2009; Gu et al., 2014, 2016) over North America and East Asia. The model has a horizontal resolution of 36 km and 30 vertical layers in the troposphere. Meteorological fields are assimilated using the Weather Research and Forecasting (WRF) model constrained by the NCEP Climate Forecast System Version 2 (CFSv2) data (Saha et al., 2011). The anthropogenic emissions are from the emission inventory of 2010 for the Task Force on Hemispheric Transport of Air Pollution version two (HTAPv2). The biogenic isoprene emissions are calculated using the Model of Emissions of Gases and Aerosols from Nature (MEGAN v2.1) algorithm (Guenther et al., 2012). The chemical mechanism is adopted from GEOS-Chem v9.1 with updates on chemistry of aromatics (Liu et al., 2012) and isoprene (Paulot et al., 2009; Crouse et al., 2011). Transport schemes (advection, convection, and turbulent mixing) are implemented following previous work (Grell, 1993; Walcek, 2000; Hong et al., 2006).

The simulation experiment in this study uses REAM outputs for July 2011. The results are evaluated against DISCOVER-AQ aircraft measurements during the same period of time over the Washington D.C.-Baltimore areas. Fig. 2 shows the comparison of the vertical profiles between the aircraft observations and REAM simulation. The REAM-simulated vertical profiles of NO₂, CH₂O, and O₃ are in good agreement with aircraft observations. Notably, the large vertical gradients of NO_x in the boundary layer observed during the DISCOVER-AQ 2011 campaign (Zhang et al., 2016) are well simulated by REAM. In addition, the REAM simulation is also able to reproduce the relationship between near-surface ozone (~300 m) and column-integrated CH₂O and NO₂ (Fig. 3). Schroeder et al. (2016) and Cheng et al. (2017) have reported the correlation between the column densities of O₃ and CH₂O during DISCOVER-AQ 2011. Our results show that near-surface O₃ is also correlated with CH₂O column (Fig. 3a and b) and this relationship may be exploited to derive surface O₃ indirectly from space. More evaluation of REAM simulations with DISCOVER-AQ data can be found in Cheng et al. (2017). In summary, the REAM model shows a good capacity to

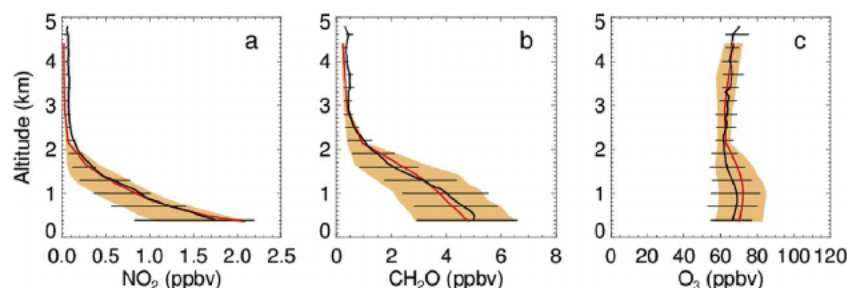


Fig. 2. Observed (black) and simulated (red) vertical profiles for NO₂, CH₂O and O₃ during the DISCOVER-AQ 2011 campaign. Standard deviations of the data are shown as horizontal lines for observations and shadings for model simulations. (For interpretation of the references to colour in this figure legend, the reader is referred to the Web version of this article.)

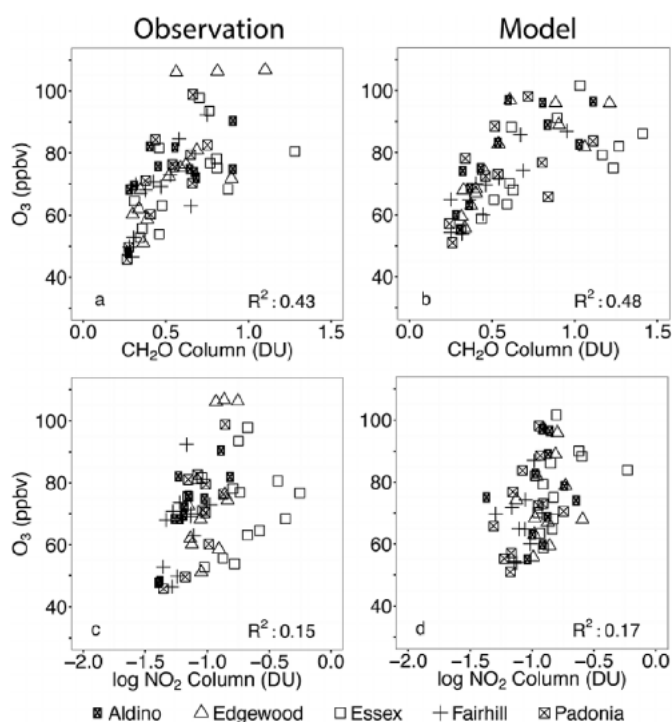


Fig. 3. Observed (a, c) and simulated (b, d) relationships between near-surface ozone and column densities of CH_2O (a, b) and NO_2 (c, d) during DISCOVER-Q 2011. Each symbol represents a daily average at a certain surface site. Data measured between 12:00 p.m.–4:00 p.m. local time are used. Near-surface ozone is measured at the lowest altitude (~ 300 m) of each vertical profile sampling by the aircraft. Note that NO_2 data are log-transformed.

reproduce the observed variability in O_3 , NO_2 and CH_2O and is an appropriate tool for the simulation experiment.

It is noteworthy that the simulation experiment approach here implicitly assumes that the statistical relationship derived from the REAM model has explanatory power similar to that in the real atmosphere. Although this assumption is supported by the evaluation with DISCOVER-AQ 2011 observations (Figs. 2 and 3), it is limited in time and location. More observations (possibly from future geostationary satellites) are needed to better characterize the spatial and temporal variation in the relationship between surface ozone and column NO_2 and CH_2O .

3. Results and discussion

3.1. ISR statistical predictors

In the simulation experiment, we tested various statistical models to describe the relationship between column observations and surface ozone. As introduced in Section 2.2, we calculate the parameters of the statistical models using the surface ozone and column data at hypothetical surface sites in the simulation experiment. In this section, we will present results with a SSD of 252 km (i.e., the hypothetical surface sites are assigned every 7 grids in both east-west and north-south directions). The impact of SSD on performance of the ISR method will be discussed in Section 3.3.

The results from the simulation experiment show that tropospheric NO_2 and CH_2O columns are informative for deriving surface ozone (Fig. 4). It is interesting to note that although both the observations and the model show a strong correlation ($R^2 = 0.43$) between surface O_3 and CH_2O columns during DISCOVER-AQ 2011 (Fig. 3) over the Washington-Baltimore area, our simulation experiment indicates a much smaller overall explanatory power ($R^2 = 0.15$) in a larger domain (i.e., the eastern US), which is mainly caused by the spatially varying

relationship between surface ozone and CH_2O columns. The relationship tends to be stronger in isoprene-abundant regions and weaker in anthropogenic emission dominated regions (Cheng et al., In preparation). In addition, the explanatory power of NO_2 is only moderate over both the DISCOVER-AQ region and the whole domain, although ozone production is thought to be NO_x -limited over much of the eastern US (Duncan et al., 2010; Martin et al., 2004). This is mainly due to the fact that a simple statistical relationship between co-located surface ozone and NO_2 columns cannot reflect the ozone production upwind. The additional complication by lightning NO_2 aloft (Zhao et al., 2009) may further deteriorate the explanatory power of NO_2 columns.

Including both CH_2O and NO_2 column densities as the ISR predictors (Linear) improves the performance over either the “ CH_2O ” or “ NO_2 ” cases (Fig. 4), indicating that CH_2O and NO_2 column densities contain independent pieces of information for surface ozone. For example, the NO_2 column densities, highly varying on a regional scale, may be useful for characterizing the urban to rural gradient. On the other hand, the CH_2O column densities are featured with less regional gradient but are informative about day-to-day variations in photochemistry, especially over the isoprene-abundant regions. The inclusion of second order terms (Full), which can partly account for the non-linear response of ozone production to the NO_x and VOCs amounts, further improves the performance (Fig. 4).

In this study, we only show simulation experiment results using column measurements made at 1:00 p.m. local time. Additional analyses show that we are able to achieve similar performances if we use columns measured in other afternoon hours (1:00 p.m.–4:00 p.m.) (Fig. S1 in the supplement). Furthermore, these afternoon columns may be averaged to reduce the impact of random measurement errors (See discussions in Section 3.4).

3.2. Added value to surface observations

The simulation experiment shows that CH_2O and/or NO_2 column densities (Section 3.1) have some capability to predict surface ozone (R^2 : 0.15–0.36; RMSE: 10.9–12.7 ppbv). However, none of the ISR methods using only column predictors outperforms “SI” (R^2 : 0.53; RMSE: 9.3 ppbv), in which the surface observations are interpolated spatially. By incorporating the information from surface observations with the spatially interpolated correction field, the post-correction procedure (the “+SI” cases) significantly improves the overall performance (Fig. 4). For example, “Full + SI” (R^2 : 0.64; RMSE: 8.2 ppbv) outperforms both “Full” (R^2 : 0.36; RMSE: 10.9 ppbv) and “SI” (R^2 : 0.53; RMSE: 9.3 ppbv) at an SSD of 252 km. The spatial distributions of the R^2 and RMSE at the SSD of 252 km (Fig. 5) show that the performance of SI generally decreases away from the hypothetical surface sites (perfect performance shown as red dots in the R^2 plot and blue dots in the RMSE plot). By utilizing the information of tropospheric column observations of NO_2 and CH_2O , “Full + SI” significantly improves the prediction performance at locations away from surface sites. The increase in R^2 and decrease in RMSE from “SI” to “Full + SI” demonstrate that the ISR method we propose can add values to the surface observation network to derive gap-free surface ozone fields.

Fig. 6 shows the added value (increase in R^2 and decrease in RMSE) of column observations as a function of SSD. It shows that all the ISR predictors discussed in Section 3.1 can improve the performance over the SI case, which only utilizes surface observations. Consistent with Section 3.1, the largest improvement over the SI case is found in the “Full + SI” case, followed by “Linear + SI”, “ NO_2 +SI”, and “ CH_2O + SI” cases. Fig. 6 also shows that the added values by the ISR predictors generally increase with the SSD, mainly because the performance of the “SI” method decreases rapidly with increasing SSDs (i.e., sparser surface sites), indicating that the ISR method can be an effective tool to derive surface O_3 mixing ratios where surface sites are sparse. Section 3.3 gives a detailed discussion on the impact of SSD.

The comparison between the “truth” and results from the ISR

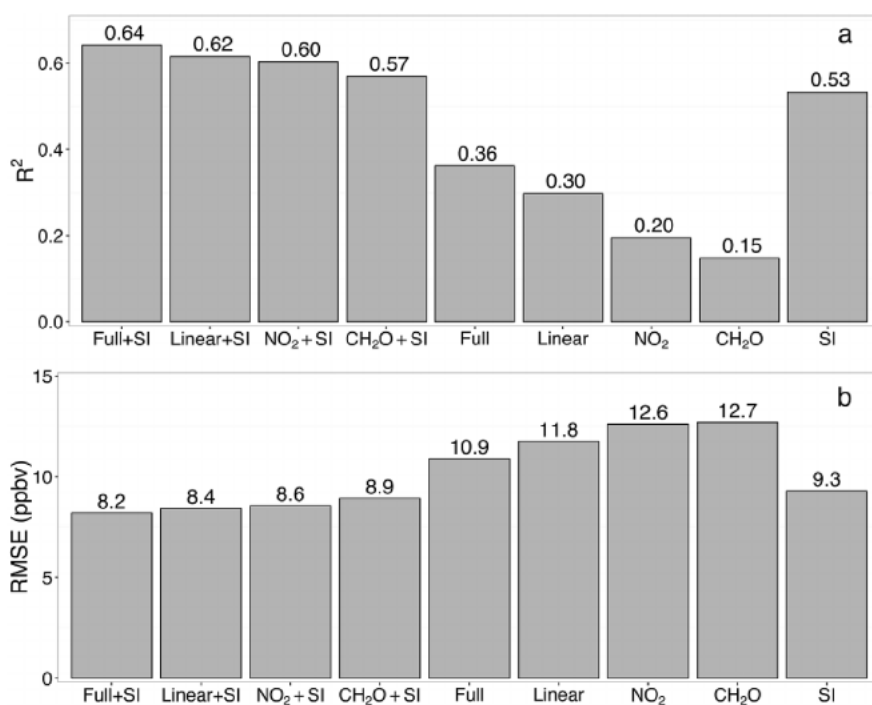


Fig. 4. Prediction performance (R^2 and RMSE) of different statistical models at an SSD of 252 km.

methods for July 1 and 16 (Fig. 7) provides insights in understanding the added values of the ISR methods. In comparison with the “truth”, the “Full” method (without post-correction with surface observations) captures the local variability (i.e., the contrast between hot spots and surroundings) quite well but shows systematic biases on regional scales (e.g., the regional overestimation in the South on July 16). This is due to the fact that the ISR statistical predictors are applied in the whole domain for the whole month, and therefore are unable to account for the day-to-day and region-to-region variability in the O_3 - NO_2 - CH_2O relationship. On the other hand, the “SI” method captures the regional mean quite well, but misses detailed features in spatial distribution, especially at locations distant from surface sites. The “Full + SI”

method possesses the merits of both “SI” and “Full” methods and generates a bias-reduced gap-free surface O_3 field. Fig. 7 illustrates the impressive performance by the “Full + SI” method in capturing the spatial distribution of surface ozone on July 1 ($R^2 = 0.80$; RMSE = 5.6 ppbv) and July 16 ($R^2 = 0.59$; RMSE = 7.8 ppbv).

3.3. Impact of surface site distances

This section examines the impact of SSD on the ISR method. As described in Section 2.1, we use data at all the hypothetical surface sites to derive the domain-wide relationship between surface ozone and tropospheric column densities of CH_2O and NO_2 . Additional surface

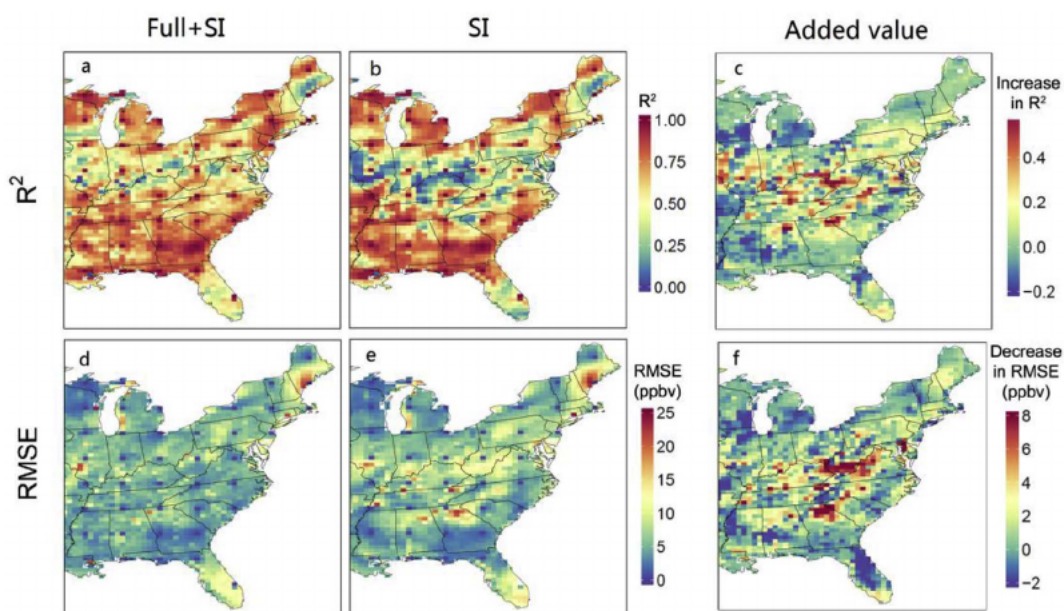


Fig. 5. Spatial distributions of the prediction performance and the added values by the ISR method at an SSD of 252 km a and b plot the R^2 for “Full + SI” and “SI”. c plots the increase in R^2 from “SI” to “Full + SI”. d and e plot the RMSE for “Full + SI” and “SI”, and f plots the reduction in RMSE from “SI” to “Full + SI”.

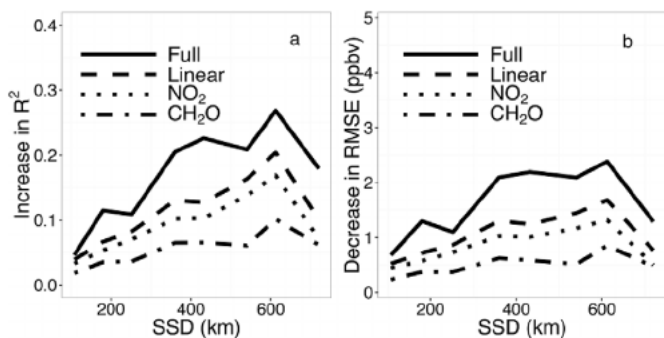


Fig. 6. The added values (increase in R^2 (a) and decrease in RMSE (b)) of the ISR method to the SI method of surface observations as a function of SSD.

sites add only marginal information to the regression model. The spatial and temporal variability of the retrieved surface ozone from the ISR method is largely determined by the variability in the column densities of CH_2O and NO_2 . Therefore, the performance of the ISR method (without post-correction with surface observations) is insensitive to the proximity of surface sites. As shown in Fig. 8, the overall R^2 and RMSE for the “Full” method remain at ~ 0.3 and ~ 11 ppbv, respectively, in a large range of SSDs (72–720 km). On the other hand, the variability of surface O_3 in the “SI” method relies on ozone observations at nearby surface sites. Therefore, the results from the “SI” method is highly dependent on the proximity of surface sites. Fig. 8 shows that the performance of the SI method improves steadily as SSD decreases from 600 km to 72 km.

By post-correcting the ISR method with surface observations, the “Full + SI” method includes the complementary information from accurate surface measurements and gap-free column measurements. Therefore, “Full + SI” is able to outperform both “Full” and “SI” at all SSDs (Fig. 8). It is noteworthy that the information from column measurements can still increase the overall R^2 by ~ 0.1 and decrease the overall RMSE by ~ 1 ppbv at an SSD of 180 km, demonstrating that tropospheric column observations of CH_2O and NO_2 add values to surface observations even when the surface sites are relatively dense.

3.4. Impact of column measurement uncertainties

The simulation experiment in the above sections uses the model-simulated tropospheric column densities of CH_2O and NO_2 for the indirect retrievals of surface ozone, which is analogous to using accurate satellite observations with no measurement (and retrieval) errors.

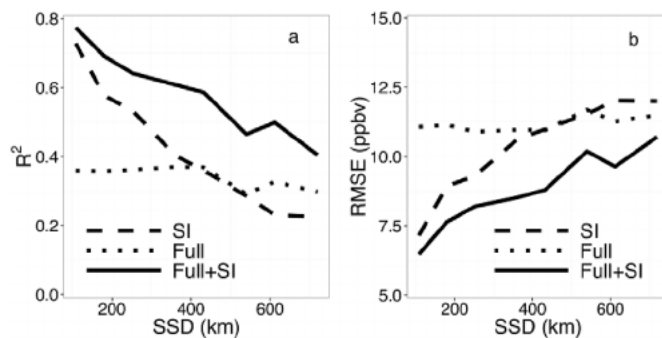


Fig. 8. Performance of the “Full + SI”, “Full”, “SI” methods as a function of SSD.

This assumption will certainly be unrealistic in operation. To assess the impact of measurement errors on the ISR method, we apply random Gaussian errors to the simulated CH_2O and NO_2 tropospheric columns and use the perturbed column densities to conduct the ISR method. The standard deviations of the random errors are 2×10^{15} and 0.5×10^{15} molecules $\cdot\text{cm}^{-2}$ for CH_2O and NO_2 tropospheric columns, respectively, based on the designed precisions for a TEMPO single retrieval (Chance et al., 2013). As expected, the superimposed noises degrade the performance of both “Full” and “Full + SI” methods (Fig. 9), but the “Full + SI” method is still able to provide added values to surface observations at an SSD of 252 km (Increase in R^2 : 0.05; Decrease in RMSE: 0.5 ppbv). These results show that the ISR method can still be useful if the measurement and retrieval errors for CH_2O and NO_2 tropospheric columns are moderate. It should be noted that the standard deviation we assigned is based on designed precisions for a single retrieval. These random errors can be significantly reduced if we derive daily column measurements by averaging multiple daytime retrievals within the same day, which will be readily available from geostationary satellites. Fig. S1 in the supplement suggests that afternoon columns are all quite informative to surface ozone. Based on that, we conduct an additional test using averages of 5 afternoon columns (one for each hour from 12:00 p.m. to 4:00 p.m.). With reduced random errors, this test show performance metrics (R^2 : 0.62; RMSE: 8.5 ppbv) comparable to those of using accurate 1:00 p.m. column measurements. This result indicates that the temporal variation within the afternoon columns induces little complication to the method.

4. Summary

Moderate correlations between near-surface ozone mixing ratios and

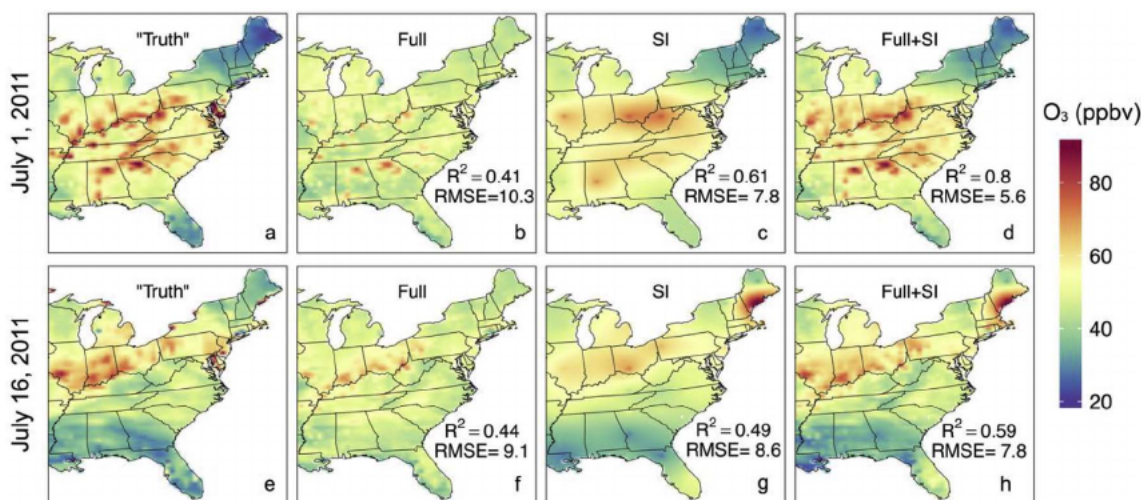


Fig. 7. Ground-level ozone prediction using the “Full”, “SI”, and “Full + SI” methods at an SSD of 252 km for July 1 and July 16 of 2011.

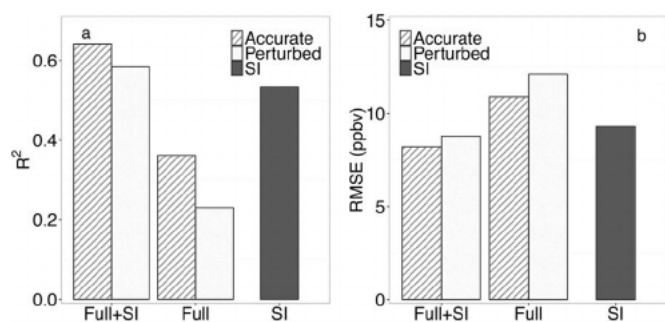


Fig. 9. Impact of column measurement uncertainties on the performance at an SSD of 252 km.

tropospheric column densities of CH_2O and NO_2 have been found in recent aircraft campaigns, suggesting that satellite measurements of these columns may provide valuable information to indirectly retrieve surface ozone. In this study, we conducted a simulation experiment to demonstrate the potential of using satellite column measurements of NO_2 and CH_2O to derive surface ozone fields, using REAM model outputs as the “true” atmosphere. The simulation experiment shows that the tropospheric NO_2 and CH_2O column densities can be effective predictors for surface ozone, but using column densities alone cannot outperform spatial interpolation of surface observations if surface sites are dense enough (< 400 km). Compositing column and surface observations (correct the surface ozone prediction by column densities with spatially interpolating biases found at surface sites) leads to the best performance in deriving full spatial coverage of surface ozone fields, mainly because NO_2 and CH_2O column densities can provide information on the fine-scale spatial pattern, which is unavailable in sparse surface ozone observations. We also examined the impact of uncertainties of column measurements on the performance. We found that the uncertainties degrade the quality of indirect retrievals. For example, the R^2 value using the “Full + SI” method decreases by ~ 0.05 with specified measurement errors, but still outperform the “SI” method by ~ 0.05 at an SSD of 252 km, suggesting that column measurements can still be useful to supplement surface observations when satellite measurement uncertainties are moderate and surface sites are sparse. Furthermore, we show that it is also viable to reduce the impact of random measurement errors by averaging multiple afternoon retrievals, which will only be available from geostationary satellites.

The goal of this study is to demonstrate the concept of ISR and provide the basis for designing operational assimilation systems for exploitation of these data. Because of the setup of our simulation experiment, we do not characterize complications such as cloud contamination or surface site representativeness, which are factors to be considered in an operational system. Furthermore, in the current study, we use statistical relationships between surface ozone and co-located tropospheric NO_2 and/or CH_2O column densities and apply the relationships over the whole domain. This simple statistical model cannot fully account for the complex physical and chemical processes that link surface ozone with column NO_2 and CH_2O . The approach may be further improved in the future by introducing more sophisticated statistical modeling, or, alternatively, using a chemical transport model as the forward model to better exploit the information content in high-quality column measurements of tropospheric NO_2 and CH_2O .

Acknowledgements

The research was supported by the NASA ACMAP Program (NNX13AK18G and NSSC17K0269).

Appendix A. Supplementary data

Supplementary data related to this article can be found at <http://dx.doi.org/10.1016/j.atmosenv.2018.02.044>.

References

- Avnery, S., Mauzerall, D.L., Liu, J., Horowitz, L.W., 2011. Global crop yield reductions due to surface ozone exposure: 1. Year 2000 crop production losses and economic damage. *Atmos. Environ.* 45, 2284–2296.
- Bak, J., Kim, J.H., Liu, X., Chance, K., Kim, J., 2013. Evaluation of ozone profile and tropospheric ozone retrievals from GEMS and OMI spectra. *Atmos. Meas. Tech.* 6, 239–249.
- Beer, R., 2006. TES on the aura mission: scientific objectives, measurements, and analysis overview. *IEEE Trans. Geosci. Rem. Sens.* 44, 1102–1105.
- Boersma, K.F., Eskes, H.J., Dirksen, R.J., van der A, R.J., Veeffkind, J.P., Stammes, P., Huijnen, V., Kleipool, Q.L., Sneep, M., Claas, J., Leitão, J., Richter, A., Zhou, Y., Brunner, D., 2011. An improved tropospheric NO_2 column retrieval algorithm for the ozone monitoring instrument. *Atmos. Meas. Tech.* 4, 1905–1928.
- Brunekreef, B., Holgate, S.T., 2002. Air pollution and health. *Lancet* 360, 1233–1242.
- Chance, K., Liu, X., Suleiman, R.M., Flittner, D.E., Al-Saadi, J., Janz, S.J., 2013. Tropospheric Emissions: Monitoring of Pollution (TEMPO). 88660D-88660D-88616.
- Cheng, Y., Wang, Y., Zhang, Y., Chen, G., Crawford, J.H., Kleb, M.M., Diskin, G.S., Weinheimer, A.J., 2017. Large biogenic contribution to boundary layer O_3 -CO regression slope in summer. *Geophys. Res. Lett.* 44.
- Cheng, Y., Wang, Y., Zhang, Y., Crawford, J.H., Diskin, G.S., Weinheimer, A.J., 2018. Estimator of surface ozone using formaldehyde and carbon monoxide concentrations over the eastern United States in summer. (In preparation).
- Choi, Y., Wang, Y., Zeng, T., Cunnold, D., Yang, E.-S., Martin, R., Chance, K., Thouret, V., Edgerton, E., 2008. Springtime transitions of NO_2 , CO, and O_3 over North America: model evaluation and analysis. *J. Geophys. Res.: Atmos.* 113, D20311.
- Crouse, J.D., Paulot, F., Kjaergaard, H.G., Wennberg, P.O., 2011. Peroxy radical isomerization in the oxidation of isoprene. *Phys. Chem. Chem. Phys.* 13, 13607–13613.
- Duncan, B.N., Yoshida, Y., Olson, J.R., Sillman, S., Martin, R.V., Lamsal, L., Hu, Y., Pickering, K.E., Retscher, C., Allen, D.J., Crawford, J.H., 2010. Application of OMI observations to a space-based indicator of NO_x and VOC controls on surface ozone formation. *Atmos. Environ.* 44, 2213–2223.
- Grell, G.A., 1993. Prognostic evaluation of assumptions used by cumulus parameterizations. *Mon. Weather Rev.* 121, 764–787.
- Gu, D., Wang, Y., Smeltzer, C., Boersma, K.F., 2014. Anthropogenic emissions of NO_x over China: reconciling the difference of inverse modeling results using GOME-2 and OMI measurements. *J. Geophys. Res.: Atmos.* 119, 7732–7740.
- Gu, D., Wang, Y., Yin, R., Zhang, Y., Smeltzer, C., 2016. Inverse modelling of NO_x emissions over eastern China: uncertainties due to chemical non-linearity. *Atmos. Meas. Tech.* 9, 5193–5201.
- Guenther, A.B., Jiang, X., Heald, C.L., Sakulyanontvittaya, T., Duhl, T., Emmons, L.K., Wang, X., 2012. The Model of Emissions of Gases and Aerosols from Nature version 2.1 (MEGAN2.1): an extended and updated framework for modeling biogenic emissions. *Geosci. Model Dev.* 5, 1471–1492.
- Hong, S.-Y., Noh, Y., Dudhia, J., 2006. A new vertical diffusion package with an explicit treatment of entrainment processes. *Mon. Weather Rev.* 134, 2318–2341.
- Ingmann, P., Veihelmann, B., Langen, J., Lamarque, D., Stark, H., Courrèges-Lacoste, G.B., 2012. Requirements for the GMES atmosphere service and ESA's implementation concept: sentinels-4/5 and -5p. *Rem. Sens. Environ.* 120, 58–69.
- Jin, X., Holloway, T., 2015. Spatial and temporal variability of ozone sensitivity over China observed from the ozone monitoring instrument. *J. Geophys. Res.: Atmos.* 120, 7229–7246.
- Liu, X., Bhartia, P.K., Chance, K., Spurr, R.J.D., Kurosu, T.P., 2010. Ozone profile retrievals from the ozone monitoring instrument. *Atmos. Chem. Phys.* 10, 2521–2537.
- Liu, X., Sioris, C.E., Chance, K., Kurosu, T.P., Newchurch, M.J., Martin, R.V., Palmer, P.I., 2005. Mapping tropospheric ozone profiles from an airborne ultraviolet-visible spectrometer. *Appl. Optic.* 44, 3312–3319.
- Liu, Z., Wang, Y., Vrekoussis, M., Richter, A., Wittrock, F., Burrows, J.P., Shao, M., Chang, C.-C., Liu, S.-C., Wang, H., Chen, C., 2012. Exploring the missing source of glyoxal (CHOCHO) over China. *Geophys. Res. Lett.* 39, L10812.
- Lv, B., Hu, Y., Chang, H.H., Russell, A.G., Bai, Y., 2016. Improving the accuracy of daily $\text{PM}_{2.5}$ distributions derived from the fusion of ground-level measurements with aerosol optical depth observations, a case study in north China. *Environ. Sci. Technol.* 50, 4752–4759.
- Martin, R.V., Fiore, A.M., Van Donkelaar, A., 2004. Space-based diagnosis of surface ozone sensitivity to anthropogenic emissions. *Geophys. Res. Lett.* 31, L06120.
- Paulot, F., Crouse, J.D., Kjaergaard, H.G., Kürten, A., St Clair, J.M., Seinfeld, J.H., Wennberg, P.O., 2009. Unexpected epoxide formation in the gas-phase photooxidation of isoprene. *Science* 325, 730–733.
- Reich, P.B., Amundson, R.G., 1985. Ambient levels of ozone reduce net photosynthesis in tree and crop species. *Science* 230, 566–570.
- Saha, S., Moorthi, S., Wu, X., Wang, J., Nadiga, S., Tripp, P., Behringer, D., Hou, Y.-T., Chuang, H.-y., Iredell, M., Ek, M., Meng, J., Yang, R., Mendez, M.P., van den Dool, H., Zhang, Q., Wang, W., Chen, M., Becker, E., 2011. NCEP Climate Forecast System Version 2 (CFSv2) 6-hourly Products. Research Data Archive at the National Center for Atmospheric Research, Computational and Information Systems Laboratory, Boulder, CO.
- Schroeder, J.R., Crawford, J.H., Fried, A., Walega, J., Weinheimer, A., Wisthaler, A., Müller, M., Mikoviny, T., Chen, G., Shook, M., Blake, D.R., Diskin, G., Estes, M., Thompson, A.M., Lefer, B.L., Long, R., Mattson, E., 2016. Formaldehyde column density measurements as a suitable pathway to estimate near-surface ozone tendencies from space. *J. Geophys. Res.: Atmos.* 121, 13,088–13,112.
- Timmermans, R.M.A., Lahoz, W.A., Atti, J.L., Peuch, V.H., Curier, R.L., Edwards, D.P., Eskes, H.J., Builjtes, P.J.H., 2015. Observing system simulation experiments for air quality. *Atmos. Environ.* 115, 199–213.

- Walcek, C.J., 2000. Minor flux adjustment near mixing ratio extremes for simplified yet highly accurate monotonic calculation of tracer advection. *J. Geophys. Res.: Atmos.* 105, 9335–9348.
- Worden, J., Liu, X., Bowman, K., Chance, K., Beer, R., Eldering, A., Gunson, M., Worden, H., 2007. Improved tropospheric ozone profile retrievals using OMI and TES radiances. *Geophys. Res. Lett.* 34, L01809.
- Zhang, R., Wang, Y., He, Q., Chen, L., Zhang, Y., Qu, H., Smeltzer, C., Li, J., Alvarado, L.M.A., Vrekoussis, M., Richter, A., Wittrock, F., Burrows, J.P., 2017. Enhanced trans-Himalaya pollution transport to the Tibetan Plateau by cut-off low systems. *Atmos. Chem. Phys.* 17, 3083–3095.
- Zhang, Y., Wang, Y., 2016. Climate-driven ground-level ozone extreme in the fall over the Southeast United States. *Proc. Natl. Acad. Sci. Unit. States Am.* 113, 10025–10030.
- Zhang, Y., Wang, Y., Chen, G., Smeltzer, C., Crawford, J., Olson, J., Szykman, J., Weinheimer, A.J., Knapp, D.J., Montzka, D.D., Wisthaler, A., Mikoviny, T., Fried, A., Diskin, G., 2016. Large vertical gradient of reactive nitrogen oxides in the boundary layer: modeling analysis of DISCOVER-AQ 2011 observations. *J. Geophys. Res.: Atmos.* 121, 1922–1934.
- Zhao, C., Wang, Y., 2009. Assimilated inversion of NO_x emissions over east Asia using OMI NO₂ column measurements. *Geophys. Res. Lett.* 36, L06805.
- Zhao, C., Wang, Y., Choi, Y., Zeng, T., 2009. Summertime impact of convective transport and lightning NO_x production over North America: modeling dependence on meteorological simulations. *Atmos. Chem. Phys.* 9, 4315–4327.
- Zhao, C., Wang, Y., Yang, Q., Fu, R., Cunnold, D., Choi, Y., 2010. Impact of East Asian summer monsoon on the air quality over China: view from space. *J. Geophys. Res.: Atmos.* 115, D09301.
- Zhu, L., Jacob, D.J., Kim, P.S., Fisher, J.A., Yu, K., Travis, K.R., Mickleby, L.J., Yantosca, R.M., Sulprizio, M.P., De Smedt, I., González Abad, G., Chance, K., Li, C., Ferrare, R., Fried, A., Hair, J.W., Hanisco, T.F., Richter, D., Jo Scarino, A., Walega, J., Weibring, P., Wolfe, G.M., 2016. Observing atmospheric formaldehyde (HCHO) from space: validation and intercomparison of six retrievals from four satellites (OMI, GOME2A, GOME2B, OMPS) with SEAC4RS aircraft observations over the southeast US. *Atmos. Chem. Phys.* 16, 13477–13490.
- Zoogman, P., Jacob, D.J., Chance, K., Liu, X., Lin, M., Fiore, A., Travis, K., 2014a. Monitoring high-ozone events in the US Intermountain West using TEMPO geostationary satellite observations. *Atmos. Chem. Phys.* 14, 6261–6271.
- Zoogman, P., Jacob, D.J., Chance, K., Worden, H.M., Edwards, D.P., Zhang, L., 2014b. Improved monitoring of surface ozone by joint assimilation of geostationary satellite observations of ozone and CO. *Atmos. Environ.* 84, 254–261.
- Zoogman, P., Jacob, D.J., Chance, K., Zhang, L., Le Sager, P., Fiore, A.M., Eldering, A., Liu, X., Natraj, V., Kulawik, S.S., 2011. Ozone air quality measurement requirements for a geostationary satellite mission. *Atmos. Environ.* 45, 7143–7150.
- Zou, B., Wilson, J.G., Zhan, F.B., Zeng, Y., 2009. Air pollution exposure assessment methods utilized in epidemiological studies. *J. Environ. Monit.* 11, 475–490.